Gas Diffusion

DOI: 10.1002/anie.200902998

Transport Diffusivity of CO_2 in the Highly Flexible Metal–Organic Framework MIL-53(Cr)**

Fabrice Salles, Hervé Jobic, Aziz Ghoufi, Philip L. Llewellyn, Christian Serre, Sandrine Bourrelly, Gérard Férey, and Guillaume Maurin**

Carbon dioxide is not only one of the major greenhouse gases responsible for global warming but is also a necessary intermediate species in many existing hydrogen production processes, and its selective separation from mixtures is a key point for the development of the future world economy.[1] In the last few years, much research has concentrated on the elaboration of novel porous materials that can efficiently capture and store CO_2 at a lower energetic cost, in order to fulfill strategic objectives on energy development and environmental concerns.[2] Metal–organic framework (MOF) hybrid porous solids are promising alternatives to the most common zeolite materials for application in industrial processes based on pressure swing adsorption (PSA), which are among the most economic methods for recovering CO_2 from flue streams.[3] They combine low framework density, high adsorption capacity, and moderate selectivity, and can be generated under mild conditions. Furthermore, the special interest in such hybrid porous materials, which are built up from metal–oxygen polyhedra containing either divalent (Zn^{2+}, Cu^{2+}) or trivalent (Al^{3+}, Cr^{3+}, Fe^{3+}, etc.) cations interconnected by various organic linkers (carboxylates, phosphonates, imidazolates, etc.), stems from their higher chemical versatility compared to classical porous solids.[4] The wide range of different pore sizes, shapes, and connectivities, as well as pre- or post-synthesis modification of the organic linker molecules, make possible easy modulation of the nature of the host–guest interactions to optimize their adsorption/separation performance.[3] In addition to this large variety of chemical and structural features, an unwanted property of some MOFs is their ability to adapt their pore opening to external stimuli such as inclusion of guest molecules.[5,6] Such behavior is of both fundamental and applied interest, particularly for separation purposes.

Several experimental and theoretical investigations have shown that both rigid and flexible MOFs exhibit high CO_2 capacity.[7–11] For instance, the MOF MIL-101[8] (MIL: Materials of Institut Lavoisier) has a much higher CO_2 adsorption uptake than NaY zeolite, the most widely used zeolite in industrial PSA processes[12] (40.0 vs. 8.0 mmol g^{-1} at 50 bar and ambient temperature). Furthermore, in applications involving gas storage, besides large adsorption uptake, selectivity, or regenerability, fast diffusivity of gas molecules into the porous system is also required. Although many studies have been dedicated to adsorption equilibria, only few computational studies based on molecular dynamics (MD) simulations have been reported so far on the diffusion of CO_2 in MOFs. These theoretical investigations are restricted to rigid MOFs, which do not exhibit any structural modifications in the presence of the guest molecule. Skoulidas and Sholl[13] were the first to predict both individual and collective CO_2 dynamics in MOF-5 for a wide range of loading, by determination of the self- (D_s) and transport (D_t) diffusivity, respectively. While they found a very usual decreasing profile for the self-diffusivity with increasing CO_2 concentration, as commonly observed in many zeolite systems, the transport diffusivity is a nonmonotonic function of pore loading that was not ascribed to a real physical phenomenon. Such conclusions were also recently drawn by Babarao and Jiang,[14] who performed MD calculations on the same CO_2/MOF-5 system. Yang et al.[15] employed a similar MD approach to follow the evolution of the self-diffusivity of CO_2 as a function of pressure in IRMOF-10, IRMOF-14, and MOF-177. They reported a typical decreasing profile with absolute values for D_s one order of magnitude higher than those observed in zeolites. Unfortunately, none of these predictions have been validated, as no experimental information is available in the literature for diffusion of CO_2 in any type of MOF system.

We have now used a combination of quasi-elastic neutron scattering (QENS) measurements and MD simulations to follow, for the first time, the transport diffusivity of a probe molecule included in a highly flexible porous MOF. This dual approach recently proved to be successful in investigating the dependence on loading of the self-diffusivity of H_2 and CH_4 in

[*] Dr. F. Salles, Dr. G. Maurin
Institut Charles Gerhardt Montpellier, Université Montpellier 2
Place E. Bataillon, 34095 Montpellier cedex 05 (France)
Fax: (+33) 4-6714-4290
E-mail: gmaurin@lpmc.univ-montp2.fr
Dr. H. Jobic
Institut de Recherches sur la Catalyse et l'environnement de Lyon, Université de Lyon, CNRS (France)
E-mail: herve.jobic@ircelyon.univ-lyon1.fr
Dr. A. Ghoufi
Institut de Physique de Rennes, UMR 6251 CNRS
Université Rennes 1 (France)
Dr. P. L. Llewellyn, Dr. S. Bourrelly
Laboratoire Chimie Provence
Universités d'Aix-Marseille I,II et III - CNRS (France)
Dr. C. Serre, Prof. G. Férey
Institut Lavoisier, UMR CNRS 8180
Université de Versailles Saint-Quentin-en-Yvelines (France)

[**] This work was supported by French program ANR CO_2 "NoMAC" (ANR-06-CO2-008). We thank the Institut Laue-Langevin (Grenoble, France) for the neutron beam time, Dr. M. M. Koza for his help, and the CINES for computational facilities.

Supporting information for this article is available on the WWW under http://dx.doi.org/10.1002/anie.200902998.

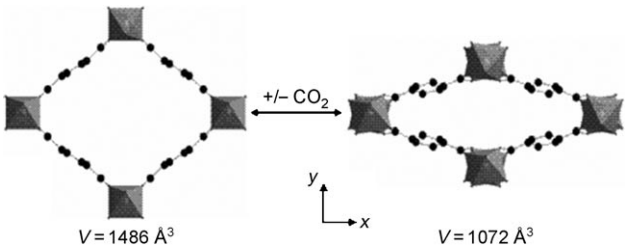

Figure 1. Structural switching of the MIL-53(Cr) system on CO_2 adsorption between large-pore (space group *Imcm*) and narrow-pore forms (space group *C*2/*c*).

rigid MOFs.[16–18] A further step here consists of elucidating the complex transport diffusion mechanism of CO_2 in MIL-53(Cr), which was selected as the most atypical MOF system for its ability to breathe in the presence of guest molecules.[19] We previously reported that this solid, built up from chains of octahedra sharing μ_2-OH vertices linked by terephthalate moieties, shows a unique large expansion/contraction of its pore size on adsorption of CO_2.[20] This behavior corresponds to two consecutive reversible structural transitions from a large-pore (LP) to a narrow-pore (NP) form at very low CO_2 loading, and from the NP to the LP form at higher CO_2 concentration. This structural switching (Figure 1) implies a 38% change in unit-cell volume, from 1072 (NP) to 1486 $Å^3$ (LP). Furthermore, both of these transitions are accompanied by a mixed-phase (NP/LP) domain whose composition varies with CO_2 pressure to give the pure NP or LP form. From a modeling standpoint, we have successfully captured these large structural modifications in MD simulations by deriving a new force field to accurately describe the interactions within the MIL framework.[21] More recently, we also developed an analytical "phase-mixture" model that can predict the fractions of NP and LP forms present in the transition zone.[22] Such major theoretical progress allows 1) long MD runs based on a robust MIL-53(Cr) framework/CO_2 force field to be conducted, and 2) the possible coexistence of the NP and LP structural forms during CO_2 adsorption to be taken into account. Both of these points are crucial for accurately probing the transport properties in host systems showing a structural phase transition induced by the guest molecules. Our joint MD-QENS strategy thus offers a unique opportunity to address for the first time the dynamics of a probe molecule in a host material which undergoes guest-assisted structural transitions.

In situ QENS measurements were performed at 230 K on the time-of-flight spectrometer IN6 at the Institut Laue-Langevin. Since the cross section of CO_2 is totally coherent, QENS monitors the transport diffusion of the adsorbate.[23] To reduce scattering from the MOF framework, a fully deuterated analogue of MIL-53(Cr) was prepared by following the synthetic and activation procedure previously described[19] but with deuterated terephthalic acid as reactant, while the hydrogen atoms of the μ_2-OH bridges were exchanged with deuterium by stirring in boiling D_2O after activation. On IN6, an incident neutron energy of 3.12 meV ($\lambda = 5.1$ Å) was applied to give a wave-vector transfer range of $Q = 0.27$–1.1 $Å^{-1}$. Different detectors were grouped in order to obtain satisfactory counting statistics, and spectra displaying Bragg peaks of the MIL-53(Cr) framework were removed. Because of the complex evolution of Bragg scattering as a function of loading, due to structural changes, only a few groupings could be selected. Most of them are situated at low Q, so that diffusion coefficients could be derived, but no details on the diffusion mechanism, jump length, and residence time could be obtained. Time-of-flight spectra were converted to energy spectra. The line shape of the elastic energy resolution could be fitted by a Gaussian function, whose half-width at half-maximum (HWHM) varied from 40 μeV at low Q to 45 μeV at high Q. After recording the scattering of the evacuated MIL-53(Cr) sample, five different CO_2 quantities determined by volumetry were adsorbed in situ, that is, 1.0, 2.5, 3.7, 5.2, and 7.4 CO_2 molecules per unit cell (u.c.), which cover the range of loading in which the MIL-53(Cr) framework exhibits the two reversible structural switchings. The structural changes of the porous solid were monitored by following the evolution of the characteristic Bragg peaks of both NP and LP forms of MIL-53(Cr) at 230 K as a function of the investigated CO_2 loading (Figure S1, Supporting Information). These observations evidenced that in the initial stage of adsorption, the MIL-53(Cr) system initially in its LP form starts to switch to the NP version. Further, one observes an NP/LP phase mixture with a fraction of the LP form that decreases with increasing CO_2 loading up to 3.7 CO_2/u.c. and then increases from 5.2 to 7.4 CO_2/u.c. This structural behavior on CO_2 adsorption is qualitatively consistent with that previously revealed at ambient temperature by in situ powder X-ray diffraction patterns.[20]

The QENS spectra recorded at 230 K for the second and fourth loadings are shown in Figure 2 for selected Q values. The measured intensities are presented in terms of the dynamical structure factor $S(Q,\omega)$, where $\hbar Q$ and $\hbar\omega$ are the momentum and energy transfers, respectively. The residual intensity measured at low Q values, before the first Bragg peak, is decreased on CO_2 adsorption, so that a negative elastic contribution appears in Figure 2a,b. The contribution due to CO_2 could nevertheless be determined, because the broadenings due to the diffusing molecules are large compared with the instrumental resolution. However, the statistics are not sufficient to analyze the profiles in detail, in order to estimate whether the diffusion is one- or three-dimensional. The transport diffusivities D_t were derived in the Fickian regime, where the broadening due to CO_2 varies as $D_t Q^2$. The values are reported in Figure 3a, and the estimated error is 50%. One observes a nonmonotonic evolution of D_t as function of CO_2 loading with a maximum, while the values only vary by a factor slightly larger than two over the whole range. This peculiar behavior can be attributed to structural switching between the NP and LP forms and to the large variation of the thermodynamic correction factor over the whole investigated range of loading. These D_t values are similar to those previously predicted for other MOFs[12,13] and about one order of magnitude larger than those previously measured in various zeolites by QENS experiments.[24,25] For the first investigated loading (1 molecule/u.c.) no broadening could be measured, that is, diffusivity is lower than 5×

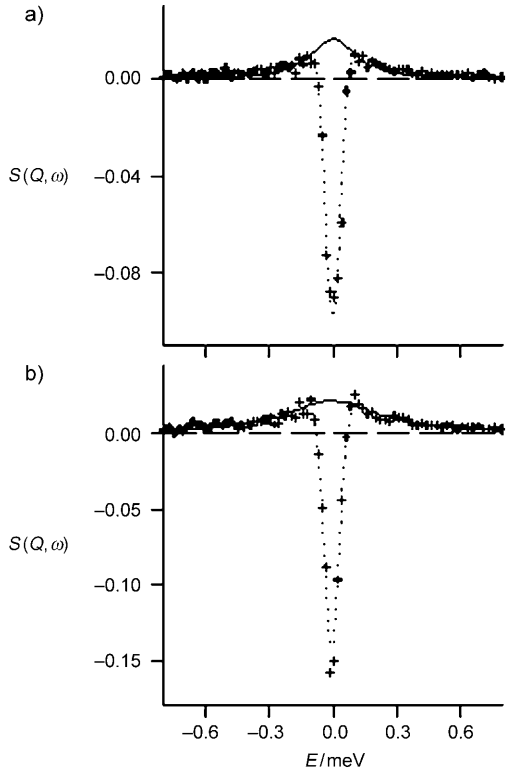

Figure 2. Comparison between experimental (crosses) and fitted (solid lines) QENS spectra; the negative elastic intensity due to MIL-53(Cr) is indicated by a dotted line. Concentrations of CO_2: a) 2.5 molecules per unit cell and b) 5.2 molecules per unit cell ($Q = 0.35$ Å^{-1}).

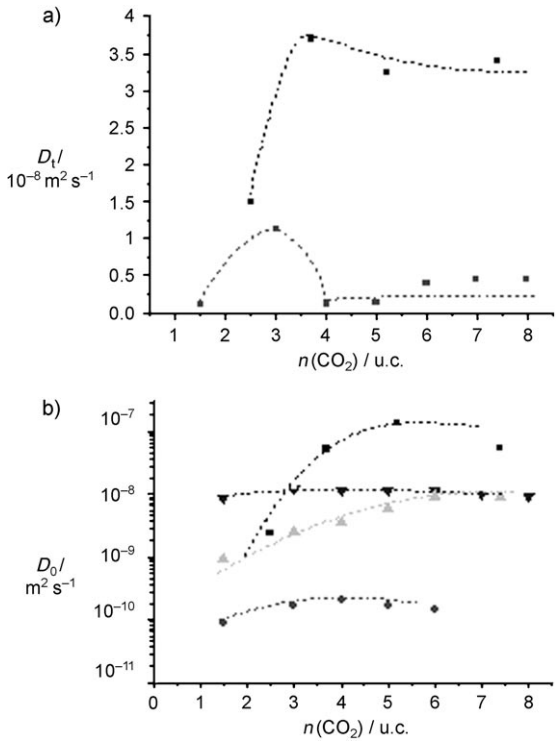

Figure 3. Comparison between a) experimental (■) and simulated (■) D_t as a function of CO_2 loading. b) Simulated D_0 for the rigid NP (●) and rigid LP forms (▼) for our composite approach (▲) and experimental data (■).

10^{-9} m^{2}s^{-1}, which suggests that this first CO_2 molecule only diffuses in the NP form.

The activation energy for transport diffusion was obtained for a CO_2 concentration of 5.2 molecules/u.c., by measuring spectra at three different temperatures. The thus-obtained value of 9.7 kJ mol^{-1} is higher than those previously reported in zeolites (5.1 and 6.3 kJ mol^{-1} in silicalite and NaY, respectively),[24,25] which means that the interactions between CO_2 and the μ_2-OH groups at the MIL-53(Cr) surface are rather strong, as previously shown by microcalorimetry and Monte Carlo calculations.[26] The corrected diffusivities D_0 can further be determined by correcting the transport diffusivities by the thermodynamic correction factors, calculated from the experimental adsorption isotherm measured at 230 K (Figures S3 and S5, Supporting Information) by means of Equation (1) where the partial derivative involving the

$$D_t(c) = D_0(c)\left(\frac{d\ln p}{d\ln c}\right) \quad (1)$$

CO_2 concentration c and pressure p is defined as the thermodynamic correction factor Γ. The resulting corrected diffusivities are reported in Figure 3b for Γ values determined for the different investigated CO_2 loadings (Figure S3, Supporting Information). The corrected diffusivity increases with increasing pore loading. This increasing profile, which is much more pronounced than those previously observed in some zeolites,[24–25] is related to the unusual behavior of the thermodynamic correction factor, which reaches values of less than 1 for loadings higher than 2.5 CO_2/u.c. This is different to that usually observed in zeolites, where Γ values are larger than 1.

Molecular dynamics simulations were then performed to help interpret the unusual D_t profile obtained from QENS data and further elucidate the complex transport diffusion mechanism of CO_2 at the microscopic scale. These calculations were based on our recently derived force field and DFT partial-charge models[21] (Figure S4, Tables S1 and S2, Supporting Information) for the MIL framework, which accurately describe the structural behavior of MIL-53(Cr) over the whole range of CO_2 adsorption. The adsorbate molecule was represented by an explicit rigid model in which each constituting atom is charged and considered as a Lennard-Jones center with parameters taken from Harris and Yung.[27] These CO_2 parameters were then combined with those of the MIL framework by using the Lorentz–Berthelot mixing rules. The resulting set of potential parameters for the MIL-53(Cr) framework and the host/guest interactions as well as the considered DFT partial charges for the MIL framework are summarized in Table S1 using the labels described in Figure S2 (see Supporting Information). As a preliminary step, our recently reported strategy, which combines grand canonical Monte Carlo (GCMC) simulations and an analytical phase-mixture model,[22] was applied at 230 K to 1) determine the fraction of the LP and NP forms in the pressure range 0–1 bar (Figure S4, Supporting Information), which follows a trend qualitatively consistent with that

obtained from the neutron diffraction patterns (Figure S1, Supporting Information), and 2) simulate a "composite" isotherm from the isotherms calculated individually for both rigid NP and LP forms, which reproduces very well the experimental adsorption isotherm extracted at 230 K by manometry measurements (Figure S3, Supporting Information). Following this validation of the thermodynamics data, MD simulations were then conducted at 230 K in the NVT ensemble (NVT = number of molecules, volume, temperature) by using the Berendsen thermostat. For each investigated CO_2 loading, the initial configurations for both the LP and NP forms were generated as described in the Supporting Information. The simulation box thus consisted of 32 unit cells of MIL-53(Cr) containing 2432 atoms loaded with 48, 96, 128, 160, 192, 224, and 256 CO_2 molecules (i.e., 1.5, 3, 4, 5, 6, 7, and 8 CO_2/u.c.) and with 48, 96, 128, 160, and 192 CO_2 molecules for the LP and NP forms, respectively, to be consistent with the range of loadings experimentally explored. Each run was performed for 2×10^7 steps with a time step of 1 fs (i.e., 20 ns) following 0.5 ns of equilibration. The Ewald summation was used to calculate the electrostatic interactions, while the short-range interactions were computed with a cutoff distance of 12 Å. Further details of the MD simulations are provided in the Supporting Information. The corrected diffusion coefficient D_0 was calculated for each CO_2 loading by using an efficient method previously described.[13] This method is based on an Einstein expression that measures the mean-square displacement (MSD) of the center of mass of the diffusive molecules [Eq. (2)] where $\langle \ldots \rangle$ denotes an ensemble

$$D_0(c) = \frac{1}{6N} \lim_{t \to \infty} \frac{1}{t} \left\langle \left\| \sum_{j=1}^{N} r_j(t) - r_j(0) \right\|^2 \right\rangle \quad (2)$$

average, N is the number of CO_2 molecules, and r corresponds to the vector position of a diffusive molecule. For each loading, the MSD curves were averaged over multiple time origins and five different MD trajectories.

The simulated values of D_0 for both NP and LP forms are reported in Figure 3b for the whole range of CO_2 loading. Clearly, both corrected diffusivities only show moderate variations with increasing CO_2 concentration, with values centered around 10^{-10} and $10^{-8}\,m^2 s^{-1}$ for the NP and LP forms, respectively. The significantly slower diffusivity simulated for the NP form is related to the highly orientational ordered arrangement of the confined CO_2 molecules into the channel, as previously shown by our DFT calculations which revealed that the CO_2 molecules are strictly aligned along the tunnel with a strong energetic double interaction with the opposing walls of the same pore.[20,28] In contrast, the diffusivity of CO_2 is faster in the LP form due to the larger space available within the pore and the weaker interaction with the CO_2/MIL-53(Cr) pore wall. This different dynamical behavior in the two forms is also consistent with the much higher activation energy simulated for a loading of 4 CO_2/u.c. in the NP form than in the LP form (23.0 vs. 13.7 $kJ\,mol^{-1}$). The calculated activation energy in the LP form is comparable to that experimentally determined for a similar loading, which supports that the measured diffusivity mainly occurs in the LP version.

A further step consisted of constructing the simulated composite evolution of D_0 as a function of the concentration c of CO_2 by using Equation (3) where X^{LP} and X^{NP} are the

$$D_0(c) = X^{LP}(c)\; D_0^{LP}(c) + X^{NP}\; D_0^{NP}(c) \quad (3)$$

fractions of the LP and NP forms, respectively, reported in Figure S4 (Supporting Information) for the different CO_2 loadings, and $D_O^{LP}(c)$ and $D_O^{NP}(c)$ correspond to the corrected diffusivities simulated individually for rigid LP and NP forms (Figure 3b). The resulting simulated composite D_0 is shown in Figure 3b. The profile compares favorably to that determined experimentally, which indicates that the CO_2 molecules occupy both NP and LP states during the observation time.

While our simulations reproduce very well the experimental value for 2.5 CO_2/u.c., they underestimate the magnitude of the increase in D_0 at higher loading. This difference can be attributed to the force field used, as no parameter adjustment was included at any point during the calculations. From these simulated D_0 values, one can deduce the transport diffusion coefficients by using Equation (1), where the thermodynamic correction factors are estimated from the simulated adsorption isotherms (Figure S3, Supporting Information). The resulting simulated D_t values are compared with the QENS data in Figure 3a. The experimental trend is thus well reproduced, while the absolute values are underestimated by our calculations. The predicted nonmonotonic profile for D_t is mainly caused by the unusual behavior of the thermodynamic correction factor, which falls below unity over a wide range of loadings (Figure S4, Supporting Information) owing to the peculiar shape of the adsorption isotherm induced by the structural transition.

In order to propose a plausible diffusion mechanism in each structural form of MIL-53(Cr), with emphasis on the confinement effect on the microscopic dynamical behavior of CO_2, 2D free energy maps through the xy plane of a given channel were calculated at different loadings for both forms of MIL-53(Cr) by using the previously reported histogram sampling method.[15] They show that in the NP form (Figure 4a), the lower-energy regions are centered on the μ_2-OH groups whatever the CO_2 concentration. This suggests that the slow diffusion of CO_2 is mainly caused by the strong interaction between the diffusive species and these hydroxy groups. Further, the minimum-energy pathways of CO_2 in this NP form, which can be approximately drawn by following the lower parts of the 2D free-energy maps, shows that the CO_2 molecules are predominantly orientated along the direction of the tunnel. It shows unambiguously that the only plausible diffusion mechanism is of 1D type along the tunnel, while displacements along the x and y directions are impossible. Moreover, inspection of the MD trajectories evidences that the sequence of the CO_2 molecules along the tunnel remains the same over time, and mutual passage is absent (Figure S6, Supporting Information). This observation suggests that a 1D single-file diffusion mechanism takes place in this NP form, as already observed in other systems with one-dimensional pore topology, including zeolites and MOFs.[29–31] This peculiar behavior is most probably due to the high orientational order of the CO_2 molecules combined with steric restrictions, as was previously pointed out by DFT calculations.[28]

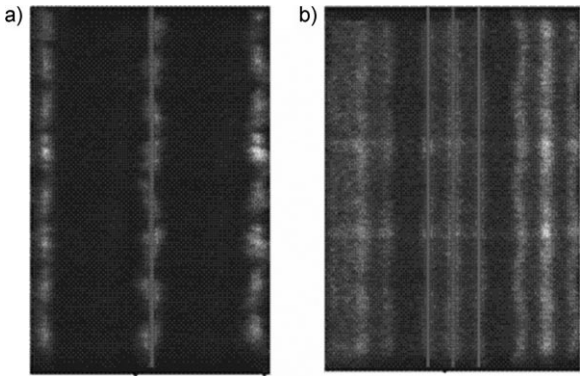

Figure 4. Typical illustration of the 1D microscopic diffusion mechanism of CO_2 obtained from 2D maps through the *xy* plane (shown in Figure 1) in a) NP ($4\,CO_2$/u.c) and b) LP ($7\,CO_2$/u.c.) forms of MIL-53(Cr). The white and black regions correspond to regions of lower and higher free energy, respectively.

As the LP form has larger pores, one would expect a different dynamical behavior for CO_2 at the microscopic scale with random motions within the pore. However, as depicted in Figure 4b, the displacements of the CO_2 molecules are mainly restricted along the direction of the tunnel, and the most favorable interactions between CO_2 and the μ_2-OH groups lead to a global 1D normal diffusion mechanism. Further, we also observed that this behavior is even more valid at higher loading ($7\,CO_2$/u.c.), where the interactions between the probe molecules tend to enhance the predominance of unidirectional diffusion along the *z* axis by sterically restricting motion in the *x* and *y* directions.

Our strategy of combining QENS experiments and MD simulations was thus able to follow for the first time the transport diffusivity of a guest molecule confined in a highly flexible MOF-type material characterized by a spectacular phase transition between two distinct structural forms. From a modeling standpoint, the great challenge was to describe accurately the diffusion process in both NP and LP forms prior to adopting a composite approach to simulate the dynamical behavior of the MIL-53(Cr) system for the whole range of CO_2 loading. From a fair agreement between the QENS and simulated data, it was then possible to understand the D_t profile and elucidate a 1D diffusion mechanism in both structural forms, whereby the diffusivity in the LP form is two orders of magnitude faster than in the NP form. We were also able to predict a single-file diffusion regime in the NP form at high loading, which was never evidenced before in any MOF-type material. Such a validated methodology is an essential tool for further understanding the dynamical behavior of flexible MOF–guest systems, which is a crucial step prior to designing novel MOFs for various applications including gas storage, gas- or liquid-phase separation, and controlled drug release.

Received: June 3, 2009
Revised: August 10, 2009
Published online: September 23, 2009

Keywords: carbon dioxide · diffusion · metal–organic frameworks · molecular dynamics · neutron diffraction

[1] R. E. Morris, P. S. Wheatly, *Angew. Chem.* **2008**, *120*, 5044; *Angew. Chem. Int. Ed.* **2008**, *47*, 4966.
[2] E. S. Kikkinides, R. T. Yang, S. H. Cho, *Ind. Eng. Chem. Res.* **1993**, *32*, 2714.
[3] F. V. S. Lopes, C. A. Grande, A. M. Ribeiro, J. M. Loureiro, O. Evaggelos, V. Nikolakis, A. E. Rodrigues, *Sep. Sci. Technol.* **2009**, *44*, 1045.
[4] G. Férey, *Chem. Soc. Rev.* **2008**, *37*, 191.
[5] G. Férey, C. Serre, *Chem. Soc. Rev.* **2009**, *38*, 1380.
[6] T. K. Maji, S. Kitagawa, *Pure Appl. Chem.* **2007**, *79*, 2155.
[7] Y. B. Bae, K. L. Mulfort, H. Frost, P. Ryan, S. Punnathanam, L. J. Broadbelt, J. T. Hupp, R. Q. Snurr, *Langmuir* **2008**, *24*, 8592.
[8] P. L. Llewellyn, S. Bourrelly, C. Serre, A. Vimont, M. Daturi, L. Hamong, G. De Weireld, J. S. Chang, D. Y. Hong, Y. K Hwang, S. H. Jhung, G. Férey, *Langmuir* **2008**, *24*, 7245.
[9] P. S. Barcia, L. Bastin, E. J. Hurtado, J. A. C. Silva, A. E. Rodrigues, B. L. Chen, *Sep. Sci. Technol.* **2008**, *43*, 3494.
[10] P. D. C. Dietzel, R. E. Johnsen, H. Fjellvag, S. Bordiaga, E. Groppo, S. Chavan, R. Blom, *Chem. Commun.* **2008**, 5125.
[11] R. Banerjee, A. Phan, B. Wang, C. Knobler, H. Furukawa, M. O'Keeffe, O. M. Yaghi, *Science* **2008**, *319*, 939.
[12] G. Maurin, P. L. Llewellyn, R. G. Bell, *J. Phys. Chem. B* **2005**, *109*, 16084.
[13] A. I. Skoulidas, D. S. Sholl, *J. Phys. Chem. B* **2005**, *109*, 15760.
[14] R. Babarao, J. Jiang, *Langmuir* **2008**, *24*, 5474.
[15] Q. Yang, C. Zhong, J. F. Chen, *J. Phys Chem. C* **2008**, *112*, 1562.
[16] N. Rosenbach, H. Jobic, A. Ghoufi, F. Salles, G. Maurin, S. Bourrelly, P. L. Llewellyn, T. Devic, C. Serre, G. Férey, *Angew. Chem.* **2008**, *120*, 6713; *Angew. Chem. Int. Ed.* **2008**, *47*, 6611.
[17] F. Salles, H. Jobic, G. Maurin, M.M. Koza, P.L. Llewellyn, T. Devic, C. Serre, G. Férey, *Phys. Rev. Lett.*, **2008**, 245901, *Phys. Rev. Lett.* **2008**, *100*, 245901.
[18] F. Salles, D. I. Kolokolov, H. Jobic, G. Maurin, P. L. Llewellyn, T. Devic, C. Serre, G. Férey, *J. Phys. Chem. C* **2009**, *113*, 7802.
[19] C. Serre, F. Millange, C. Thouvenot, M. Noguès, G. Marsolier, D. Loüer, G. Férey, *J. Am. Chem. Soc.* **2002**, *124*, 13519.
[20] C. Serre, F. Millange, C. Thouvenot, M. Noguès, G. Marsolier, D. Loüer, G. Férey, *Adv. Mater.* **2007**, *19*, 2246.
[21] F. Salles, A. Ghoufi, G. Maurin, R.G. Bell, C. Mellot-Draznieks, G. Férey, *Angew. Chem.* **2008**, *120*, 8615; *Angew. Chem. Int. Ed.* **2008**, *47*, 8487.
[22] A. Ghoufi, G. Maurin, unpublished results.
[23] H. Jobic, D. Theodorou, *Micropor. Mesopor. Mater.* **2007**, *102*, 21.
[24] D. Plant, H. Jobic, P. L. Llewellyn, G. Maurin, *Eur. Phys. J.* **2007**, *141*, 127.
[25] G. K. Papadopoulos, H. Jobic, D. N. Theodorou, *J. Phys. Chem. B* **2004**, *108*, 12748.
[26] N. A. Ramsahye, G. Maurin, S. Bourrelly, P. L. Llewellyn, T. Loiseau, C. Serre, G. Férey, *Chem. Commun.* **2007**, 3261.
[27] J. G. Harris, K. H. Yung, *J. Phys. Chem.* **1995**, *99*, 12021.
[28] N. Ramsahye, G. Maurin, S. Bourrelly, P. L. Llewellyn, C. Serre, T. Loiseau, T. Devic, G. Férey, *J. Phys. Chem. C* **2008**, *112*, 514.
[29] A. I. Skoulidas, D. S. Sholl, *J. Phys. Chem. A* **2003**, *107*, 10132.
[30] H. Jobic, K. Hahn, J. Kaerger, M. Bee, A. Tuel, M. Noack, I. Gimus, G. J. Kearley, *J. Phys. Chem. B* **1997**, *101*, 5834.
[31] L. Heinke, D. Tzoulaki, C. Chmelik, F. Hibbe, J. M. van Baten, H. Lim, J. Li, R. Krishna, J. Kärger, *Phys. Rev. Lett.* **2009**, *102*, 065901.

